ISSN 1075-7015, Geology of Ore Deposits, 2018, Vol. 60, No. 7, pp. 594–606. © Pleiades Publishing, Ltd., 2018.
Original Russian Text © N.V. Zubkova, I.V. Pekov, N.V. Chukanov, A.V. Kasatkin, D.A. Ksenofontov, V.O. Yapaskurt, S.N. Britvin, D.Yu. Pushcharovsky, 2017, published in Zapiski Rossiiskogo Mineralogicheskogo Obshchestva, 2017, No. 6, pp. 43–61.

NEW MINERALS

Redefinition of Lemanskiite: New Mineralogical Data, Crystal Structure, and Revised Formula $NaCaCu_5(AsO_4)_4Cl \cdot 3H_2O$

N. V. Zubkova[a, *], I. V. Pekov[a], N. V. Chukanov[b], A. V. Kasatkin[c], D. A. Ksenofontov[a], V. O. Yapaskurt[a], S. N. Britvin[d], and D. Yu. Pushcharovsky[a]

[a] *Geological Faculty, Moscow State University, Moscow, 119991 Russia*
[b] *Institute of Problems of Chemical Physics, Russian Academy of Sciences, Chernogolovka, Moscow oblast, 142432 Russia*
[c] *Fersman Mineralogical Museum, Russian Academy of Sciences, Leninskii pr. 18-2, Moscow, 119071 Russia*
[d] *Institute of the Earth Sciences, St. Petersburg State University, Universitetskaya nab. 7/9, St. Petersburg, 199034 Russia*
**e-mail: n.v.zubkova@gmail.com*

Received June 20, 2017

Abstract—The crystal structure of lemanskiite is determined for the first time ($R = 0.019$) and the mineral is redefined. Its chemical formula, crystal system, space group and unit-cell parameters are revised. The powder X-ray diffraction pattern of lemanskiite has been correctly indexed; the IR spectrum of an impurity-free sample has been obtained. It has been shown that the mineral is not a dimorph of lavendulan $NaCaCu_5(AsO_4)_4Cl \cdot 5H_2O$ and differs from the latter by a lower H_2O content. The studied sample was from the oxidation zone of the Perseverancia deposit, Guanako, Antofagasta, Chile. It empirical formula is $Na_{0.98}(Ca_{0.98}Sr_{0.03})_{\Sigma 1.01}Cu_{5.07}As_{3.97}O_{15.97}Cl_{1.03} \cdot 3H_2O$; the idealized formula is $NaCaCu_5(AsO_4)_4Cl \cdot 3H_2O$. The mineral is monoclinic, $P2_1/m$, $a = 9.250(2)$, $b = 10.0058(10)$, $c = 10.0412(17)$ Å, $\beta = 97.37(3)°$, $V = 921.7(3)$ Å^3, $Z = 2$. Lemanskiite represents a new structure type in the lavendulan group. Its structure is based on heteropolyhedral layers composed of clusters consisting of four edge-shared distorted Cu-centered tetragonal pyramids joined with eight AsO_4 tetrahedra, which are also linked with a Cu-centered plane squares not involved in the clusters. Interlayer edge-shared Na-centered trigonal prisms and Ca sevenfold polyhedra are linked with the heteropolyhedral layers from both sides.

Keywords: lemanskiite, lavendulan, lavendulan group, arsenate, crystal structure, oxidation zone, Perseverancia mine, Chile

DOI: 10.1134/S1075701518070115

INTRODUCTION

Lemanskiite, hydrous Cu, Ca, and Na chlorarsenate, was described as a new mineral species by Ondruš et al. (2006). It was found in the oxidation zone of the Abundancia gold deposit, Guanako ore district, Antofagasta Province, Chile. The chemical composition of this mineral was determined using electron microprobe and CHN technique; its suggested idealized formula $NaCaCu_5(AsO_4)_4Cl \cdot 5H_2O$ was identical to that of lavendulan. A single crystal X-ray diffraction study failed due to low quality of crystals. However, the differences in the powder X-ray diffraction patterns and physical properties of lavendulan and arsenate from Abundancia (Table 1) were so dramatic that it allowed identification of the latter as an individual mineral species, which is dimorphic to the former (Ondruš et al., 2006). At the same time, based on a certain similarity in the powder X-ray diffraction patterns of lemanskiite and lavendulan-group members, the authors of the referred paper reported their relatives and suggested tetragonal system (space group $P4_122$ or $P4_322$) and unit-cell parameters $a = 9.9758(4)$, $c = 36.714(1)$ Å, $V = 3653.6(2)$ Å^3, $Z = 2$ for their new mineral by analogy with original data for zdenekite $NaPbCu_5(AsO_4)_4Cl \cdot 5H_2O$, lead analog of lavendulan (Chiappero and Sarp, 1995). Having revised many museum samples marked as "lavendulan" from various locations, Ondruš et al. (2006) found that some of the powder X-ray diffraction patterns are consistent with that of lemanskiite.

Despite the fact that lemanskiite is not an extremely rare mineral, it sometimes occurs as large (up to a few mm) individuals, and their clusters reach a few cm across, the crystal structure of this arsenate has not yet been solved and insight into its symmetry and unit cell parameters were based only on powder X-ray diffraction data. Therefore, the powder X-ray diffraction data were the main criterion for attributing the mineral with the composition of the metal–chlorarsenate part as $NaCaCu_5(AsO_4)_4Cl$ to lavendulan or lemanskiite.

Table 1. Comparative data for lemanskiite and lavendulan

Mineral	Lemanskiite		Lavendulan
Formula	$NaCaCu_5(AsO_4)_4Cl \cdot 3H_2O$		$NaCaCu_5(AsO_4)_4Cl \cdot 5H_2O$
Symmetry	Monoclinic		Monoclinic
Space group	$P2_1/m$		$P2_1/n$
a, Å	9.284	9.260**	10.011
b, Å	10.018	10.029**	19.478
c, Å	10.058	10.031**	10.056
β, °	97.25	97.30**	90.37
V, Å	928	924**	1961
Z	2	2	4
Strongest reflections in powder X-ray diffraction pattern: *d*, Å – *I*	9.21–100		9.72–100
	4.990–14		5.003–7
	4.607–17		4.865–16
	4.393–12		4.449–7
	3.135–14		3.156–6
	2.928–14		3.110–9
	2.699–14		2.968–9
	2.606–14		2.752–7
	2.491–12		
Measured density, g/cm^3	3.78*		3.54
Reference	This study (except density)		Anthony et al., 2000; Giester et al., 2007; ICDD 49-1856

* Data taken from (Ondruš et al., 2006);
** Calculated for holotype lemanskiite from *d*-spacings of reflections in powder X-ray diffraction pattern reported by Ondruš et al. (2006) and *hkl* values obtained from our structure data

However, some points in (Ondruš et al., 2006) raise serious questions. This particularly applies to the formula of lemanskiite and the compositional identity of the mineral to lavendulan. Data on the crystal structure of lavendulan published in 2007 confirmed its layered nature. Giester et al. (2007) unambiguously confirmed the chemical formula of lavendulan $NaCaCu_5(AsO_4)_4Cl \cdot 5H_2O$ and found a pseudotetragonal monoclinic unit cell with $V = 1961$ Å^3 (Table 1). Note that it is nearly identical in dimensions and volume to the unit cell of zdenekite (1964 Å^3), which also appeared to be pseudotetragonal monoclinic but not tetragonal (Zubkova et al., 2003). The doubled cell volume of lavendulan [to bring it into correspondence with the aforementioned initial tetragonal model for zdenekite (Chiappero and Sarp, 1995)] is 3922 Å^3, which is significantly different from the 3654 Å^3 published for lemanskiite (Ondruš et al., 2006). Lavendulan and lemanskiite also differ greatly in the major basal *d*-spacing (9.7–9.9 and 9.18 Å, respectively) and measured density (3.54 and 3.78 g/cm^3, respectively) (Anthony et al., 2000; Ondruš et al., 2006; JCPDS-ICDD ##31-1280, 49-1857, and 51-1491). It would be difficult to accept that $NaCaCu_5(AsO_4)_4Cl \cdot 5H_2O$ dimorphs with related layered structures sufficiently differ in these parameters. Taking into account interlayer water molecules in lavendulan-type structures, the different degree of hydration of these arsenates is the most probable reason for such distinctions (Zubkova et al., 2003; Pushcharovsky et al., 2004; Giester et al., 2007). In this case, lavendulan should be more highly hydrated than lemanskiite; therefore, they are not dimorphs.

This study has confirmed this assumption. We found the hydrous mineral with the composition of the metal–chlorarsenate part as $NaCaCu_5(AsO_4)_4Cl$ (according to electron microprobe data), whose powder X-ray diffraction pattern is very similar to that of original lemanskiite (Table 2), which made it possible to attribute our sample precisely to this mineral species. A single crystal suitable for X-ray structure analysis was picked out of this material, and the obtained structural model was refined by the Rietveld method using powder X-ray diffraction data. This paper focuses on redefining lemanskiite with respect to the chemical formula and crystallographic parameters as well as a structural description and comparative crystal chemistry of this mineral.

Table 2. Powder X-ray diffraction data for lemanskiite

Perseverancia mine, Antofagasta, Chile: our data				Holotype (Ondruš et al., 2006)		Our data
I_{obs}	d_{obs}	I_{calc}*	d_{calc}**	I_{obs}	d_{obs}	*hkl*
2	10.00	0.5	9.958	2	9.946	001
				9	*9.600***	
100	9.21	100	9.174	100	9.177	100
11	7.06	8	7.058	2	7.037	011
8	6.77	6	6.762	2	6.746	110
1	6.38	0.5	6.353			101
3	5.848	5	5.857	<1	5.908	$\bar{1}11$
				1	*5.584*	
1	5.374	1	5.363			111
14	4.990	5, 5	5.003, 4.979	2	4.976	020, 002
17	4.607	7, 11	4.632, 4.587	3, 32	4.639, 4.374	$\bar{1}02$, 200
12	4.393	11, 3	4.392, 4.385	3, 2	4.205	120, $\bar{2}01$
		0.5	4.204	2	4.167, 4.119	$\bar{1}12$
10	4.173	10, 3	4.170, 4.158	10, <1	4.004	210, 102
2	3.989	4	3.977	2	3.774	201
1	3.844	0.5	3.840	<1	3.529	112
3	3.531	2	3.529	<1	3.373	022
2	3.387	2	3.381	<1	3.317	220
2	3.322	1	3.319	<1		003

SAMPLE

The lemanskiite sample studied here came from the oxidation zone of the Percevarencia deposit located in the Guanako district at the Abundancia deposit. This mineral fills fractures in vein quartz as bright blue lamellar crystals up to 2 mm in length with perfect cleavage parallel to (100), which locally occur as radial rosettes or chaotic aggregates up to 5 mm across. The frequently split crystals are lath-shaped and flattened parallel to [100] ({100} is the major face) and are commonly intergrown along the {100} faces (Fig. 1).

CHEMICAL COMPOSITION

The chemical composition (cations and chlorine) of lemanskiite from the Percevarencia mine was determined on a Jeol JSM-6480LV scanning electron microscope equipped with an INCA-Energy 350 EDS (ATW-2 window) with an acceleration voltage of 20 kV, current intensity of 0.7 nA, and a beam diameter 5 μm. The following standards were used NaCl (Na, Cl), microcline (K), $CaMoO_4$ (Ca), SrF_2 (Sr), $CuFeS_2$ (Cu), and FeAsS (As). The water content was not determined by a direct method due to insufficient material, so it was calculated from structural data: three H_2O molecules per formula (see below).

The chemical composition of lemanskiite from the Perseverancia mine is, wt %: 2.92 Na_2O, 0.02 K_2O, 5.32 CaO, 0.26 SrO, 38.99 CuO, 44.03 As_2O_5, 3.54 Cl, 5.22 H_2O_{calc}, –0.80 $-O=Cl_2$; the total is 99.50. The contents of other elements with atomic numbers >6 were below the detection limits of the electron microprobe. The empirical formula calculated on the basis of 20 O + Cl is $Na_{0.98}(Ca_{0.98}Sr_{0.03})_{\Sigma 1.01}Cu_{5.07}As_{3.97}O_{15.97}Cl_{1.03} \cdot 3H_2O$. As is seen, it is very close to the idealized formula $NaCaCu_5(AsO_4)_4Cl \cdot 3H_2O$ obtained from the structure data. The studied lemanskiite crystals are quite homogenous in composition.

INFRARED SPECTROSCOPY

The infrared (IR) spectra of lemanskiite and lavendulan samples pressed with KBr in pellets (Fig. 2) were measured on a Bruker Optics ALPHA FTIR spectrometer within the wavenumber range 360–3800 cm^{-1}, at a resolution of 4 cm^{-1}; the number of scans was 16. A pure KBr disc was used as a reference. The position (cm^{-1}) and assignment of the bands in the IR spectrum of lemanskiite from Perseverancia are as follows (spectrum (a) in Fig. 2; s is strong band, w is weak band, sh is shoulder): 3551, 3441, 3419, 3303, 3223 (O–H stretching vibrations of H_2O molecules), 1734w, 1621, 1580w (bending vibrations of H_2O mole-

Table 2. (Contd.)

Perseverancia mine, Antofagasta, Chile: our data				Holotype (Ondruš et al., 2006)		Our data
I_{obs}	d_{obs}	I_{calc}*	d_{calc}**	I_{obs}	d_{obs}	*hkl*
3	3.256	3	3.258			$\bar{1}03$
8	3.194	13, 4	3.198, 3.177	<1, <1	3.202, 3.173	122, 202
14	3.135	14, 0.5	3.135, 3.098	3, 1	3.135, 3.120	130, $\bar{1}13$
6	3.066	3	3.058	15	3.059	300
8	3.004	9	3.001	2	3.007	103
				<1	*2.977*	
		0.5	2.953	<1	2.954	131
14	2.928	27, 1	2.929, 2.924	5	2.924	$\bar{2}22$, 310
5	2.872	7	2.870	3	2.892	$\bar{2}03$
9	2.765	0.5	2.835	<1	2.835	301
		2, 6, 3, 0.5	2.771, 2.769, 2.766, 2.758	<1, <1	2.771, 2.752	032, $\bar{3}02$, 023, $\bar{2}13$
8	2.727	3	2.730	<1	2.716	$\bar{1}23$
14	2.699	8, 9, 15	2.707, 2.698, 2.682	<1, <1	2.698, 2.692	$\bar{1}32$, 230, 222
14	2.606	12, 7	2.609, 2.602	1, 6	2.620, 2.606	320, 132
3	2.576	6	2.573			123
12	2.491	5, 4, 6, 3	2.501, 2.490, 2.489, 2.485	2	2.4915	040, 004, $\bar{2}23$, $\bar{1}04$
5	2.461	4, 3, 3	2.468, 2.459, 2.450	1	2.4654	302, 321, $\bar{2}32$
3	2.416	2, 2	2.423, 2.413	<1	2.4084	$\bar{3}22$, 140
2	2.400	3	2.396			312
1	2.360	0.5	2.364			$\bar{1}41$
2	2.303	2	2.300			232
1	2.267	2, 2	2.300, 2.264			232, 223
1	2.239	1	2.231	<1	2.2355	133
2	2.171	1	2.170	<1	2.1811	$\bar{3}23$
2	2.140	3, 1	2.142, 2.130	<1, <1	2.1626, 2.1361	$\bar{4}12$, $\bar{3}32$
2	2.108	1, 1, 1, 1	2.117, 2.111, 2.102			241, 124, $\bar{2}24$
1	2.087	1	2.090	<1	2.0834	$\bar{4}21$
1	2.058	1	2.057			$\bar{2}42$
1	2.036	1	2.036			214
1	2.024	1	2.022			$\bar{3}14$
2	1.994	1	1.994			421
4	1.959	1, 1, 3	1.962, 1.961, 1.955			051, $\bar{1}15$, 150
3	1.950	0.5, 1, 0.5	1.953, 1.950, 1.950			015, 412, 323
3	1.924	1, 0.5, 0.5, 0.5, 1	1.930, 1.929, 1.921, 1.920, 1.919			$\bar{3}41$, $\bar{1}51$, 143, 224, $\bar{2}05$
2	1.911	0.5, 0.5, 0.5	1.909, 1.909, 1.909			134, 151, $\bar{3}24$
1	1.894	1	1.890			430
1	1.854	1	1.856			$\bar{3}42$
1	1.834	0.5, 0.5	1.837, 1.832			$\bar{1}52$, $\bar{4}32$
1	1.806	1, 2, 2	1.805, 1.803, 1.798	4, 1	1.8049, 1.8009	510, 152, $\bar{5}02$
6	1.765	2, 6, 7, 1	1.773, 1.764, 1.763, 1.757	1	1.7643	125, 044, $\bar{1}44$, 342
1	1.724	3, 0.5	1.723, 1.714	3, 2	1.7219, 1.7216	520, 053
3	1.696	0.5, 0.5, 0.5, 2	1.699, 1.693, 1.693, 1.692			$\bar{4}24$, $\bar{4}41$, 252, $\bar{5}22$
3	1.672	3, 1, 2	1.674, 1.671, 1.668	<1	1.6694	350, $\bar{1}06$, 060

Table 2. (Contd.)

Perseverancia mine, Antofagasta, Chile: our data				Holotype (Ondruš et al., 2006)		Our data
I_{obs}	d_{obs}	I_{calc}*	d_{calc}**	I_{obs}	d_{obs}	*hkl*
1	1.656	1	1.654	<1	1.6506	502
1	1.608	3	1.609			$\bar{4}05$
3	1.584	0.5, 0.5, 3	1.588, 1.581, 1.579			$\bar{4}34$, 062, 305
3	1.572	1, 3	1.572, 1.570	<1	1.5758	253, 522
2	1.551	2, 1, 2, 1	1.554, 1.545, 1.548, 1.547			352, $\bar{2}26$, 162, 235
1	1.532	1, 0.5	1.532, 1.529	<1, <1	1.5294, 1.5280	$\bar{4}25$, 600
2	1.510	1, 4, 2	1.514, 1.508, 1.506			$\bar{2}62$, 450, 325
1	1.479	3	1.478			$\bar{4}52$
1	1.465	0.5, 0.5	1.462, 1.462			620, $\bar{6}03$
1	1.451	2	1.452			622
2	1.447	1, 2	1.448, 1.445	<1	1.4479	$\bar{3}45$, $\bar{5}05$
1	1.437	0.5, 0.5	1.437, 1.432			$\bar{3}54$, 245
3	1.414	1, 4, 2, 2	1.416, 1.415, 1.412, 1.410			405, $\bar{1}55$, -05, 452
1	1.390	1, 1	1.390, 1.388	<1	1.3889	630, $\bar{5}25$

* Reflections with $I \geq 0.5$ are given for calculated powder X-ray diffraction pattern.
** Calculated from single crystal X-ray diffraction data.
*** Close in position to major reflection of lavendulan.
Three reflections of X-ray diffraction pattern of original lemanskiite given in (Ondruš et al., 2006) not indexed in obtained unit cell are italicized.

cules), 928, 875sh, 838s, 813s, 791s (stretching vibrations of AsO_4^{3-} anions), 539s, 483s, 439 (bending vibrations of AsO_4^{3-} anions and possibly Cu–O stretching vibrations). Weak bands at 1225, 1102, and 629 cm^{-1} are referred to minor sulfate anions.

The IR spectrum of lavendulan (spectrum (c) in Fig. 2) is close to that of lemanskiite in the region of the AsO_4^{3-} vibrations, but is strongly different from the latter in the region of the H_2O vibrations (1500–3600 cm^{-1}). Lavendulan is particularly characterized by a stronger

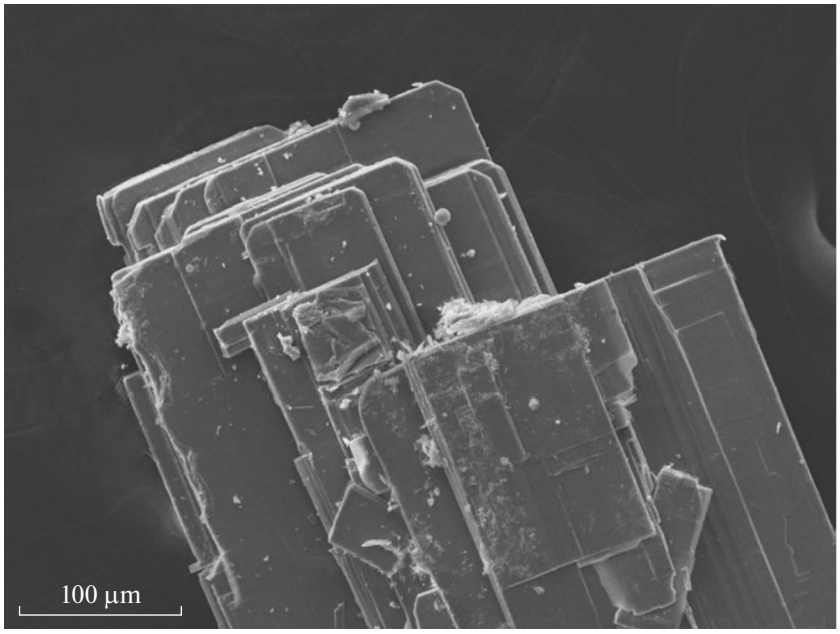

Fig. 1. Secondary electron image of parallel intergrowth of lemanskiite crystals from Perseverancia mine, Guanaco, Antofagasta, Chile.

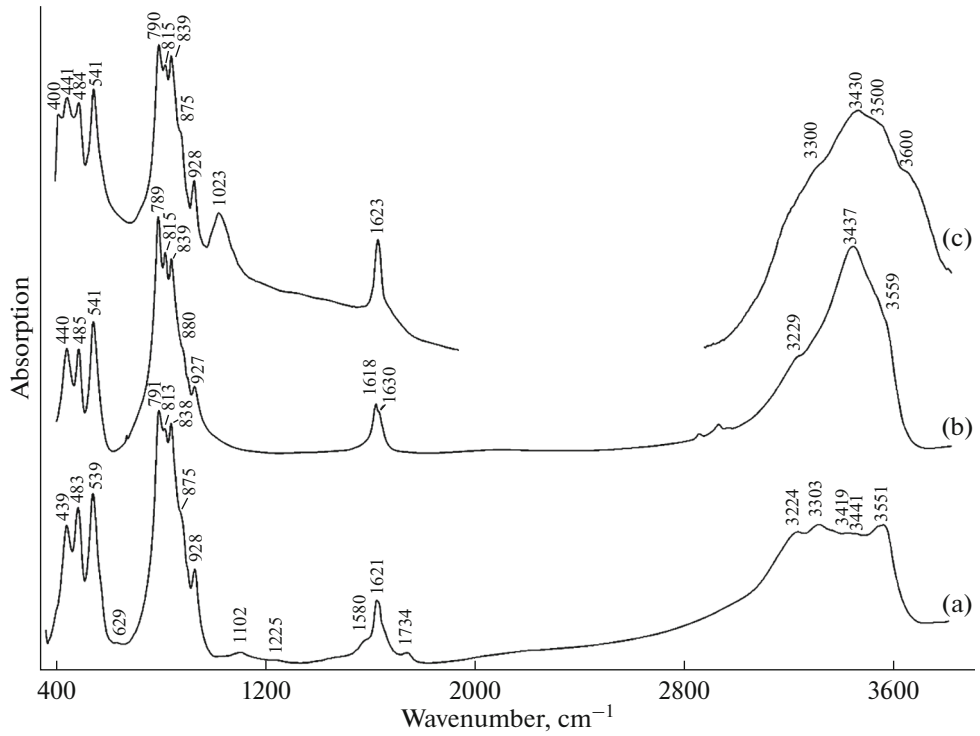

Fig. 2. IR spectra of (a) lemanskiite from Perseverancia mine, Guanaco, Chile, studied here; (b) sample from Abundancia mine, Guanaco, taken from (Ondruš et al., 2006), and (c) lavendulan from Serpieri mine, Lavrion, Greece (Chukanov, 2014).

absorption in the region of the O–H stretching vibrations. The position of absorption bands of lemanskiite and lavendulan are dramatically different in this region. An additional band at 400 cm^{-1} in the lavendulan spectrum may correspond to the stretching vibrations of a C–O–Na fragment belonging to the apex-shared Ca- and Na-centered polyhedra (see below). A relatively weak band at 1023 cm^{-1} in the spectrum of lavendulan from Lavrion is attributed to PO_4^{3-} anions which, substitute for arsenate anions in the mineral structure.

X-RAY CRYSTASLLOGRAPHY

A single crystal X-ray diffraction study of lemanskiite was performed at room temperature with an XCaliburS CCD diffractometer with MoK_α radiation ($\lambda = 0.71073$ Å] for a crystal 0.04 × 0.08 × 0.14 mm in size for a full sphere of the reciprocal space. The experimental data were processed with the CrysAlisPro v. 1.171.37.35 software package (Agilent Technologies, 2014). The monoclinic unit cell parameters of the single crystal are: $a = 9.250(2)$, $b = 10.0058(10)$, $c = 10.0412(17)$ Å, $\beta = 97.37(3)°$, $V = 921.7(3)$ Å^3. The crystal structure was determined by direct methods and refined in space group $P2_1/m$ using the SHELX-97 software package (Sheldrick, 2008). Unfortunately, the insufficient quality of the crystal (a certain mosaicity with slightly disoriented blocks) prevented a low residual factor: the final R value was 11.50% for 635 unique reflections with $I > 2\sigma(I)$. However, satisfactory equivalent displacement parameters and interatomic distances, as well as bond valence calculations, indicate a correct structural model.

The crystal structure of lemanskiite was refined based on the powder X-ray diffraction pattern and verified by the Rietveld method (we also checked for other possible polytypes of the mineral taking into account its layered structure). The powder X-ray diffraction data were collected on a Rigaku R-AXIS RAPID II diffractometer with CoK_α radiation (λ = 1.79021 Å) in the Debye–Shererr geometry (d = 127.4 mm). The initial data from the cylindrical detector were integrated, and a complete profile of the X-ray diffraction pattern was obtained with the osc2tab software package (Britvin et al., 2017). The structural model obtained from the single-crystal data was accepted as the initial one, and the JANA2006 program (Petříček et al., 2006) was used for refinement. The atomic displacement parameters were fixed. The pseudo-Voigt function was used to model the peak profiles. The data for minor admixed quartz were used in the calculation, which made it possible to take into account several weak reflections. The ratio of these two minerals in the powder sample is 97.9% lemanskiite and 2.1% quartz. The refinement resulted in the following final residual factors: R_{wp} 1.90%, R_p 1.45%, and R_{obs} 1.88%. The experimental and calcu-

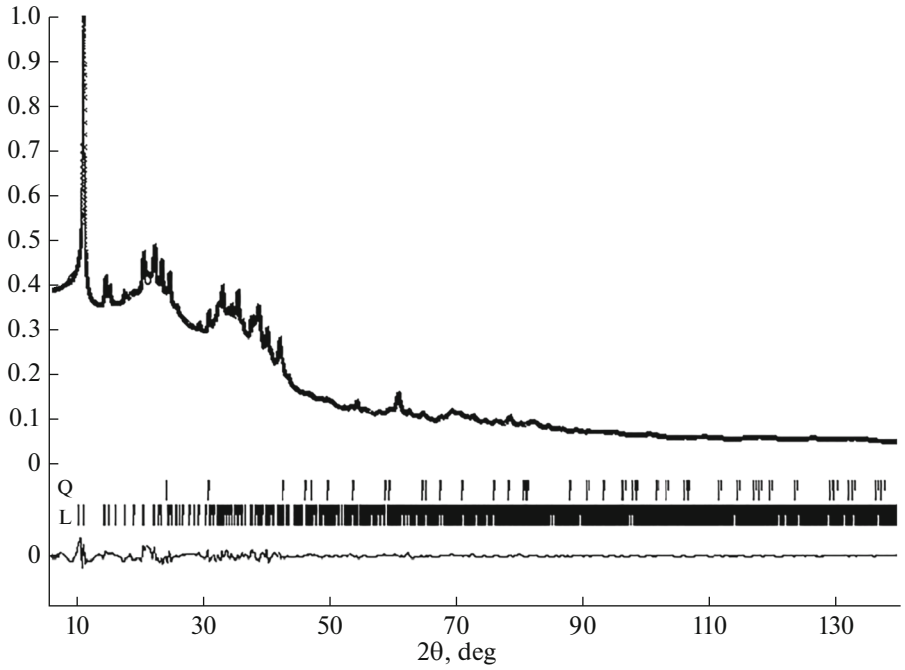

Fig. 3. Observed (asterisks) and calculated (line) powder X-ray diffractions patterns of multiphase pattern containing lemanskiite and quartz. Vertical dashes show positions of reflections in calculated pattern [upper part for quartz (Q) and lower part for lemanskiite (L)]. Diagram at bottom of figure illustrates difference between intensities of observed and calculated patterns.

lated powder X-ray diffraction patterns of the sample containing lemanskiite and quartz are shown in Fig. 3.

In Table 2 the reflections of the powder X-ray diffraction pattern of lemanskiite (with an intensity ≥1% and ≥0.5% for the experimental and calculated patterns, respectively) were indexed according to the structure data; quartz reflections were excluded (Table 2).

Table 3 gives the crystallographic parameters, data of the single crystal and powder X-ray experiments, and refinement parameters of the lemanskiite structure; Table 4 lists the atomic coordinates and displacement parameters; Table 5 presents the interatomic distances; and Table 6 gives the calculated bond valences.

CRYSTAL STRUCTURE AND COMPARATIVE CRYSTAL CHEMISTRY

Lemanskiite represents a new structural type, but it has a substantial crystal chemical relation to the other lavendulan-group members (Giester et al., 2007) and structurally related minerals and synthetic compounds. The crystal structure of lemanskiite shown in Fig. 4 is based on heteropolyhedral layers parallel to (100) and consisting of Cu^{2+}-centered polyhedra and AsO_4 tetrahedra. Clusters composed of four edge-shared Cu fivefold polyhedra, which are distorted tetragonal pyramids [Cu(1–3)] with Cl atom as the shared apex, are identified within the layers. The Cu–Cl distances are longer than the Cu–O distances: 2.64–2.73 and 1.90–2.01 Å, respectively (Table 5). Eight AsO_4 tetrahedra are joined to each cluster of four Cu fivefold polyhedra via oxygen vertices: four tetrahedra above and four beneath; each tetrahedron shares two vertices with two Cu fivefold polyhedra of one cluster and one vertex with Cu polyhedron of the neighboring cluster. The fourth vertex of each AsO_4 tetrahedron is linked with a Cu(4)-centered polyhedron not involved in the discussed clusters. In contrast to the other lavendulan-group members in which this Cu site centers tetragonal pyramid with oxygen atom of water molecule at distant fifth apex $CuO_4(H_2O)$, lemanskiite has a plane square $Cu(4)O_4$ here. The major building unit of the heteropolyhedral layer in the structure of lemanskiite and lavendulan is shown in Figs. 5a and 5b, and these layers are shown in Figs. 5c and 5d.

It is noteworthy that similar to lavendulan and its structural analogues zdenekite and sampleite $NaCaCu_5(PO_4)_4Cl \cdot 5H_2O$, each layer in the structure of lemanskiite can be described in tetragonal symmetry. This is consistent with the initial insight into the mineral symmetry (Ondruš et al., 2006). However, like other lavendulan-group members (Zubkova et al., 2003; Giester et al., 2007), neighboring heteropolyhedral layers in the structure of lemanskiite are moved relative to one another, which results in symmetry lowered to monoclinic.

The Na and Ca cations are arranged in the structure of lemanskiite in trigonal prisms and sevenfold polyhedra, respectively. These polyhedra are joined to

Table 3. Crystallographic parameters, single-crystal and powder X-ray diffraction data, and refined parameters of crystal structure of lemanskiite

Crystallographic parameter	Data of single-crystal experiment	Data of powder experiment
Formula	$NaCaCu_5(AsO_4)_4Cl \cdot 3H_2O$	
Symmetry, space group, Z	Monoclinic, $P2_1/m$,2	
Unit cell parameters, Å/°	$a = 9.250(2)$	$a = 9.2838(13)$
	$b = 10.0058(10)$ $\beta = 97.37(3)$	$b = 10.0184(7)$ $\beta = 97.248(8)$
	$c = 10.0412(17)$	$c = 10.0578(9)$
V, Å^3	921.7(3)	927.99(17)
Calculated density*, g/cm^3	3.70	3.67
Temperature	293(2) K	
Diffractometer	Xcalibur S CCD	Rigaku R-AXIS RAPID II
Radiation; λ, Å	MoK_a; 0.71073	CoK_α; 1.79021
$\theta_{min/max}$, °	2.82/28.28	3.00/70.00
Scanning ranges	$-12 \le h \le 12$	
	$-13 \le k \le 13$	
	$-12 \le l \le 12$	
Number of observed/unique reflections	6057/1941	
Number of unique reflections with $I > 2\sigma(I)$	635	
Residual factors	$R1$ 0.1150	R_{wp} 0.0190
	w$R2$ 0.2139 [$I > 2\sigma(I)$]	R_p 0.0145
		R_{obs} 0.0188
$\Delta\rho_{max/min}$, e/Å^3	1.99/−2.07	0.57/−0.54

* For idealized formula.

the heteropolyhedral layers on both sides via edges common with Cu fivefold polyhedra. In the structure of lemanskiite, the Na and Ca polyhedra linked to the neighboring Cu–As–O–Cl layers share edges Ow(1)–Ow(1) in the interlayer space (Fig. 6a) in contrast to lavendulan, in which Na- and Ca-centered polyhedra have a common vertex (Fig. 6b).

DISCUSSION

Thus, lavendulan and lemanskiite are not dimorphs and differ in the degree of hydration. A decreased number of water molecules per formula unit from five in lavendulan and its structural analogues (zdenekite and sampleite) to three in lemanskiite results in: (1) a slightly different topology of the heteropolyhedral layer, in particular, in the disappearance of the fifth apex in the copper polyhedron, which is not involved in clusters, and this polyhedron is reduced from a tetragonal pyramid $CuO_4(H_2O)$ in lavendulan to a plane square CuO_4 in lemanskiite and (2) the transition from corner-shared polyhedra of large Ca and Na cations in lavendulan to edge-shared polyhedra in lemanskiite. Thus, the structure becomes substantially more compact owing to the shorter distance between heteropolyhedral layers, which is ~9.7 and ~9.2 Å in lavendulan and lemanskiite, respectively. This affects the values of the basal (i.e., perpendicular to heteropolyhedral layers or close to such normal) unit cell parameter (b and a in lavendulan and lemanskiite, respectively) and, therefore, the values of the basal d-spacings (in d_{0k0} and d_{h00} in lavendulan and lemanskiite, respectively). This difference is most evident in the d spacings of the first reflection of these series: $d_{010} = 9.7–9.8$ Å in lavendulan and $d_{100} \sim 9.2$ Å in lemanskiite. It is considered a reliable identification feature (especially since this is the strongest reflection in the powder X-ray diffraction pattern of both minerals, Table 1), allowing reliable identification of these minerals identical in the chemical composition of the metal–chlorarsenate part and identification of lavendulan–lemanskiite clusters.

The powder X-ray diffraction patterns of our sample from the Perseverancia mine and the holotype lemanskiite (Ondruš et al., 2006) are very similar (Table 2). Only three reflections of the holotype pattern are not indexed in the determined by us unit cell. These are reflections with $d = 9.600$ ($I = 9\%$; in our opinion, it may belong to minor admixed lavendulan), 5.584, and 2.977 Å (the intensity of two last reflections does not exceed 1%). The appreciably increased intensity of reflections 200 and 300 in the powder X-ray dif-

Table 4. Atomic coordinates, equivalent displacement parameters of cations and Cl, isotropic displacement parameters of oxygen atoms (U_{eq}/U_{iso}, Å^2 according to single crystal experiment), and site multiplicity (Q) in structure of lemanskiite

Site	x	y	z	^{U}eq/^{U}iso	Q
Na	0.713(2)	0.25	0.7071(18)	0.036(5)	2
	0.713(2)	0.25	0.7169(11)		
Ca	0.3224(10)	0.25	0.7798(9)	0.021(2)	2
	0.3243(9)	0.25	0.7812(7)		
As(1)	0.1883(3)	0.0444(2)	0.4806(3)	0.0184(8)	4
	0.1836(7)	0.0432(5)	0.4793(5)		
As(2)	0.8075(3)	0.9559(2)	0.9330(3)	0.0158(8)	4
	0.8219(6)	0.9489(6)	0.9305(5)		
Cu(1)	0.0804(4)	0.9802(3)	0.7618(4)	0.0211(10)	4
	0.0931(6)	0.9866(4)	0.7716(5)		
Cu(2)	0.0816(6)	0.75	0.5402(6)	0.0227(14)	2
	0.0612(9)	0.75	0.5292(6)		
Cu(3)	0.0809(6)	0.75	0.9861(6)	0.0210(14)	2
	0.0989(9)	0.75	0.9808(8)		
Cu(4)	0.6732(6)	0.75	0.7032(6)	0.0226(14)	2
	0.6843(11)	0.75	0.7176(10)		
Cl	0.7600(11)	0.25	0.2209(12)	0.026(3)	2
	0.7634(6)	0.25	0.2403(7)		
O(1)	0.667(2)	0.8853(19)	0.833(2)	0.025(5)	4
	0.6730(9)	0.9046(14)	0.8236(14)		
O(2)	0.808(2)	0.1252(18)	0.899(2)	0.024(5)	4
	0.7933(8)	0.1179(6)	0.9116(10)		
O(3)	0.9616(19)	0.8935(18)	0.885(2)	0.019(5)	4
	0.9682(8)	0.8806(10)	0.8744(11)		
O(4)	0.178(2)	0.0816(17)	0.640(2)	0.017(5)	4
	0.1954(8)	0.0731(2)	0.6425(5)		
O(5)	0.193(2)	0.8807(18)	0.456(2)	0.024(5)	4
	0.175(2)	0.8807(6)	0.447(2)		
O(6)	0.8062(19)	0.9218(16)	0.096(2)	0.014(4)	4
	0.8318(18)	0.8911(9)	0.0882(5)		
O(7)	0.6586(19)	0.8859(17)	0.562(2)	0.015(4)	4
	0.6716(9)	0.8911(18)	0.5816(19)		
O(8)	0.044(2)	0.1152(18)	0.385(2)	0.021(5)	4
	0.0292(11)	0.0963(13)	0.3850(13)		
Ow(1)	0.5000(19)	0.1010(17)	0.696(2)	0.019(5)	4
	0.5149(12)	0.1072(10)	0.710(3)		
Ow(2)	0.501(5)	0.25	0.964(4)	0.071(12)	2
	0.5022(8)	0.25	0.9667(7)		

Data of single crystal experiment and Rietveld refinement data are given in each first and second line of site, respectively.

fraction pattern of the original lemanskiite compared to the calculated values (Table 2) is undoubtedly caused by textured particles in the sample: the mineral cleavage is perfect parallel to (100). The unit cell parameters of the holotype sample of lemanskiite, which we calculated from *d*-spacings in the powder X-ray diffraction pattern given in (Ondruš et al., 2006) and the *hkl* indices obtained from our structure data are $a = 9.260(4)$, $b = 10.029(5)$, $c = 10.031(5)$ Å, $\beta = 97.30(4)°$, $V = 924(1)$ Å^3. The similarity of these data and those obtained for our sample (Table 1), combined with the good accuracy of the determined parameters of the "new" holotype unit cell, indicates that the model presented in this study is valid for the original lemanskiite.

The IR spectrum of the sample from Abundancia (spectrum (b) in Fig. 2) in (Ondruš et al., 2006) substantially differs in the region of O–H stretching vibra-

Table 5. Selected interatomic distances (Å) in structure of lemanskiite (data of single crystal experiment)

As(1)—O(4)	1.656(19)	As(2)—O(6)	1.67(2)
—O(5)	1.659(18)	—O(3)	1.684(18)
—O(7)	1.684(17)	—O(1)	1.69(2)
—O(8)	1.698(19)	—O(2)	1.727(19)
Cu(1)—O(4)	1.904(19)	Cu(2)—O(5)	1.931(19) × 2
—O(6)	1.930(19)	—O(8)	1.986(19) × 2
—O(3)	1.958(18)	—Cl	2.645(13)
—O(8)	1.99(2)		
—Cl	2.729(7)	Cu(4)—O(1)	1.88(2) × 2
		—O(7)	1.953(19) × 2
Cu(3)—O(2)	1.91(2) × 2		
—O(3)	2.006(19) × 2	Ca—Ow(2)	2.31(5)
—Cl	2.696(12)	—Ow(1)	2.446(18) × 2
		—O(4)	2.48(2) × 2
Na—O(5)	2.34(2) × 2	—O(6)	2.513(18) × 2
—O(2)	2.37(2) × 2		
—Ow(1)	2.46(2) × 2		

Table 6. Bond valence calculations for lemanskiite

Component	As(1)	As(2)	Cu(1)	Cu(2)	Cu(3)	Cu(4)	Ca	Na	*S*
Cl			$0.14^{x2\rightarrow}$	0.17	0.15				0.60
O(1)		1.23				$0.58^{x2\downarrow}$			1.81
O(2)		1.11			$0.54^{x2\downarrow}$			$0.21^{x2\downarrow}$	1.86
O(3)		1.25	0.47		$0.41^{x2\downarrow}$				2.13
O(4)	1.35		0.54				$0.25^{x2\downarrow}$		2.14
O(5)	1.34			$0.51^{x2\downarrow}$				$0.23^{x2\downarrow}$	2.08
O(6)		1.30	0.51				$0.23^{x2\downarrow}$		2.04
O(7)	1.25					$0.48^{x2\downarrow}$			1.73
O(8)	1.21		0.43	$0.44^{x2\downarrow}$					2.08
Ow(1)							$0.27^{x2\downarrow}$	$0.17^{x2\downarrow}$	0.44
Ow(2)							0.40		0.40
Σ	5.15	4.89	2.09	2.07	2.05	2.12	1.90	1.22	

Parameters are taken from (Brese and O'Keeffe, 1991). Bond valence sum for Cl atom can be increased owing to possible hydrogen bonding with water molecule Ow(2) [distance Cl–Ow(2) ~ 3.29 Å]; in this case bond valence sum for Ow(2) will be decreased. Similarly, decrease in bond valence sum for water molecule Ow(1) is possible owing to hydrogen bonding with atoms O(1) and O(7) [distances Ow(1)–O(1) 2.90 Å, Ow(1)–O(7) 2.81 Å]. In this case, bond valence sums for O(1)and O(7) will increase.

tions from the spectrum of the Perseverancia sample measured in this study. Strong absorption with a maximum at 3437 cm^{-1} is similar to that in the lavendulan spectrum, but the band at 400 cm^{-1} is absent. These observations suggest that the sample studied in (Ondruš et al., 2006) is a product of intermediate-stage transformation of lavendulan to lemanskiite as a result of partial dehydration. The 9.60 Å reflection close in position to the major reflection of lavendulan in the powder X-ray diffraction pattern of the Abundancia supports this suggestion. However, the presence of this reflection with an intensity of only 9% of the major lemanskiite reflection does not explain the high water content in the sample described in (Ondruš et al., 2006). The observed inconsistency between the powder X-ray diffraction pattern and IR spectrum of the Abundancia sample (and total water content in it) is most likely caused by the disordered (possibly, X-ray amorphous) phase formed at the initial stage of lavendulan dehydration. The absence of the band at 400 cm^{-1} may indicate that groups of corner-shared Ca- and Na-centered polyhedra were already broken, but most of the water is retained in the predominant disordered phase. Note that the formation of the intermediate X-ray amorphous phase (loss of long-range order of interatomic interactions at a certain stage of structural rebuilding of the single crystal to a single crystal) during dehydration of crystal hydrates and thermal

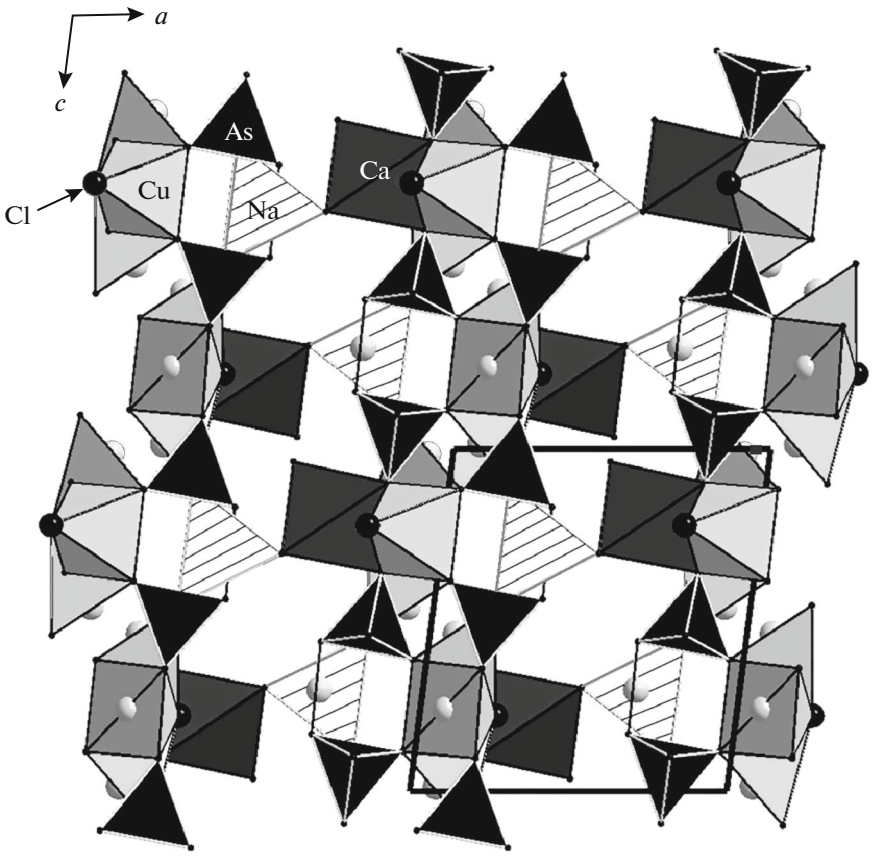

Fig. 4. Crystal structure of lemanskiite in *ac* projection. Unit cell is outlined.

transformations of crystalline compounds is well known and had been reported many times (e.g., Frost et al., 1951; Zakharov et al., 2016; Larsen et al., 2017).

Ondruš et al. (2006) reported an interesting fact: X-ray diffraction verified that lavendulan from Lavrion, Greece, once powdered transformed to lemanskiite in a few days. This phenomenon is caused by a phase transition and indicates more stable lemanskiite as compared to lavendulan (Ondruš et al., 20106). In our opinion this transformation is caused by partial dehydration, which is quicker in powder due to the much larger specific surface compared to coarse crystals, and an increased content of structural defects due to crystal powdering. It is most likely that the realization and rate of this reaction depend on air humidity.

The data obtained in this study suggest that Ondruš et al. (2006) investigated a heterogeneous material when describing the original lemanskiite. That material certainly contained lemanskiite proper, a mineral similar in structure to the one we studied (most reflections are consistent with those in the powder X-ray diffraction pattern reported by (Ondruš et al., 2006), Table 2), but in addition, lavendulan and hypothetical X-ray amorphous arsenate close in water content to lavendulan rather than to lemanskiite could have been present in the material studied by Ondruš et al. (2006). The reflection with $d = 9.60$ Å in the X-ray powder diffraction pattern could be attributed to relict (?) lavendulan, and the slightly decreased d-spacing as compared to typical lavendulan may reflect the onset of dehydration of the mineral. The impurity of lavendulan and X-ray amorphous arsenate could have been responsible for the elevated water content as determined from the bulk sample using the CHN technique. Thus, it is of interest to revise the holotype lemanskiite from the Abundancia mine in the future. In particular, an attempt can be made to study its crystal structure based on a powder sample with the Reitveld method, using as a model the structure data for the sample from the Perseverancia mine reported in this paper.

CONCLUSIONS

The key results of this study are as follows.

—The crystal structure of lemanskiite, which is a representative of a new structural type, has been determined for the first time; the symmetry and unit cell parameters of this mineral have been accurately determined; these parameters significantly differ from those determined only based on powder X-ray diffraction data.

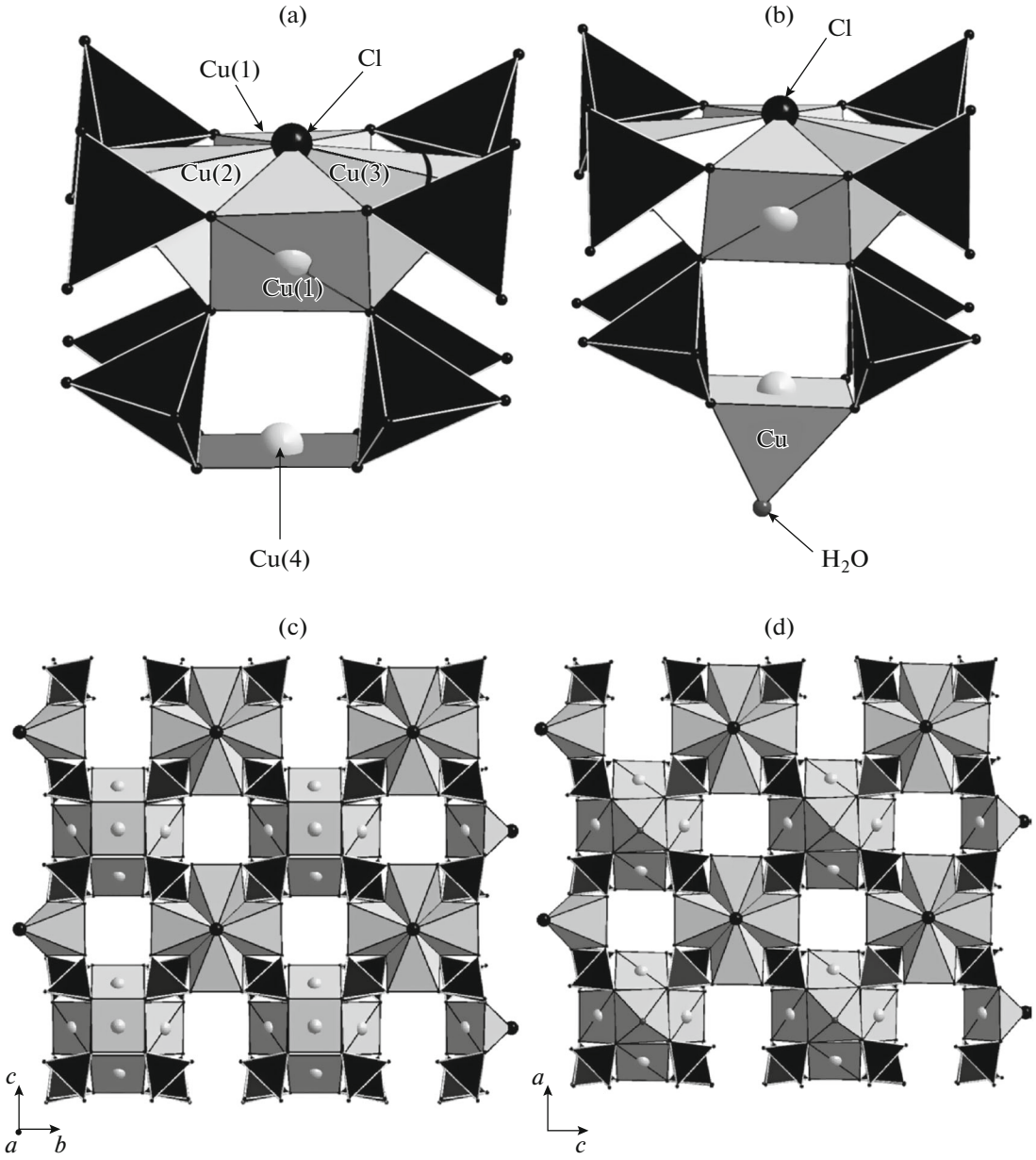

Fig. 5. Cluster consisting of Cu-polyhedra and As-tetrahedra, and Cu- polyhedron not involved in cluster in structures of (a) lemanskiite and (b) lavendulan, and Cu–As–Cl–O heteropolyhedral layers in (c) lemanskiite and (d) lavendulan, according to (Giester et al., 2007).

—The formula for lemanskiite $NaCaCu_5(AsO_4)_4Cl \cdot 3H_2O$ was refined based on structure and spectroscopic data; it was shown that lemanskiite is not a dimorph of lavendulan $NaCaCu_5(AsO_4)_4Cl \cdot 5H_2O$, as had been expected, and differs from the latter by a lower water content.

—Lemanskiite and related minerals have been compared in terms of their crystal chemistry; the topological differences in the structures of this arsenate and more highly hydrated lavendulan-group members have been demonstrated.

—The proper powder X-ray diffraction pattern of lemanskiite indexed based on structure data and the IR spectrum of an impurity-free sample has been published for the first time.

ACKNOWLEDGMENTS

The mineralogical and single crystal X-ray diffraction studies and crystal structure determination were supported by the Russian Foundation for Basic Research (project no. 17-05-00179). The powder X-ray diffraction study carried out at the Center of

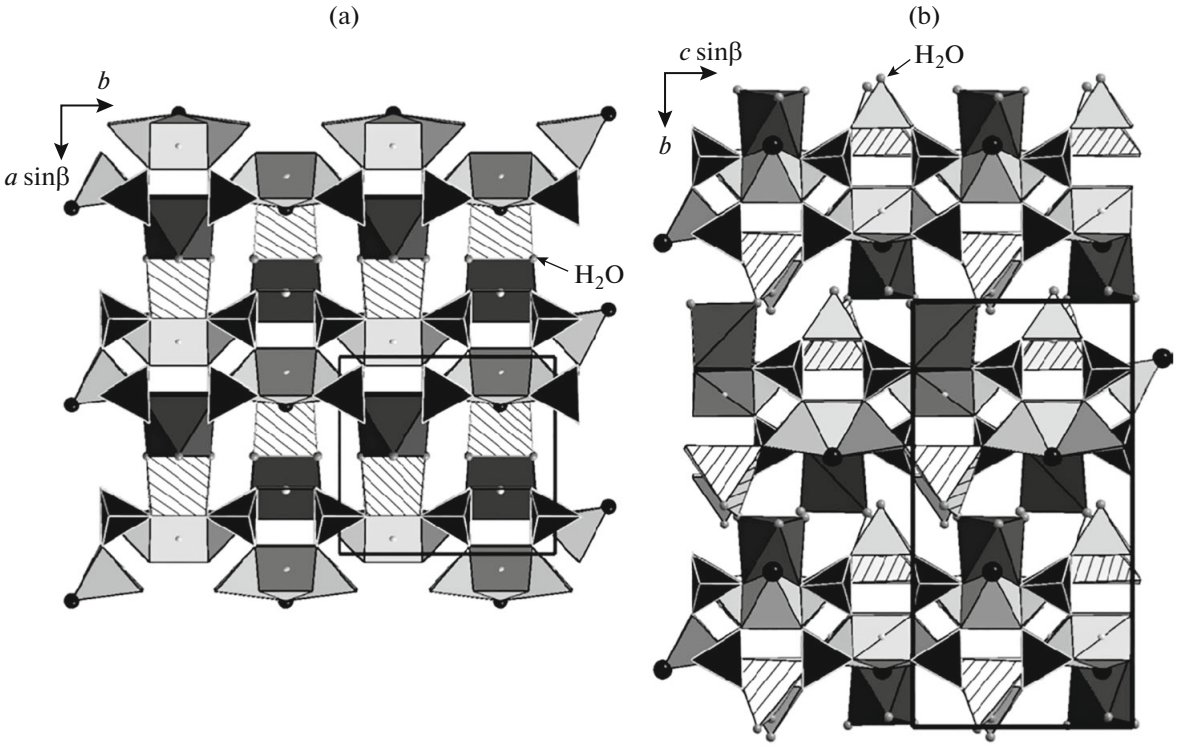

Fig. 6. Crystal structures of (a) lemanskiite and (b) lavendulan, drawn after (Giester et al., 2007). Polyhedra and atomic position are same as in legend for Fig. 4. Unit cells are outlined.

X-ray Diffraction Studies at St. Petersburg State University was supported by the Russian Science Foundation (project no. 14-17-00071).

REFERENCES

Agilent Technologies. Crysalispro Software System, Version 1.171.37.35. 2014, Oxford: Agilent Technologies UK ltd, 2014

Anthony, J.W., Bideaux, R.A., Bladh, K.W., and Nichols, M.C., *Handbook of Mineralogy. IV. Arsenates, Phosphates, Vanadates*, Tucson: Mineral Data Publishing, 2000.

Brese, N.E. and O'Keeffe, M., Bond-valence parameters for solids. *Acta Crystallograph.*, 1991, vol. 47, pp. 192–197.

Britvin, S.N., Dolivo-Dobrovolsky, D.V., and Krzhizhanovskaya, M.G., Software for processing the X-ray powder diffraction data obtained from the curved image plate detector of Rigaku RAXIS Rapid II diffractometer, *Zap. Ross. Mineral. O-va,* 2017, vol. 146, no. 3, pp. 104–107.

Chiappero, P.-J. and Sarp, H., Zdenekite, NaPbCu$_5$(AsO$_4$)$_4$Cl · 5H$_2$O, a new mineral from the Cap Garonne mine, Var, France, *Eur. J. Mineral.*, 1995, vol. 7, pp. 553–557.

Chukanov, N.V., *Infrared Spectra of Mineral Species: Extended Library,* Dordrecht: Springer-Verlag, 2014.

Frost, G.B., Moon, K.A., and Tompkins, E.H., The role of amorphous intermediate products in the dehydration of certain hydrated salts, *Can. J. Chem.*, 1951, vol. 29, no. 7, pp. 604–632.

Giester, G., Kolitsch, U., Leverett, P., Turner, P., and Williams, P.A., The crystal structures of lavendulan, sampleite, and a new polymorph of sampleite. *Eur. J. Mineral.*, 2007, vol. 19, pp. 75–93.

Larsen, A.S., Rantanen, J., and Johansson, K.E., Computational dehydration of crystalline hydrates using molecular dynamics simulations, *J. Pharm. Sci.,* 2017, vol. 106, no. 1, pp. 348–355.

Ondruš, P., Veselovsky, F., Sejkora, J., Skála, R., Pažout, R., Frýda, J., Gabašová, A., and Vajdak, J., Lemanskiite, NaCaCu$_5$(AsO$_4$)$_4$Cl · 5H$_2$O, a new mineral species from theAbundancia mine, Chile, *Can. Mineral.,* 2006, vol. 44, pp. 523–531.

Petříček, V., Dusek, M., and Palatinus, L., Jana2006. *Structure Determination Software Programs–Institute of Physics,* Praha. 2006.

Pushcharovsky, D.Yu., Zubkova, N.V., Teat, S.J., Maclean, E.J., and Sarp, H., Crystal structure of mahnertite, *Europ. J. Mineral.,* 2004, vol. 16, pp. 687–692.

Sheldrink, G.M., A short history of SHELX, *Acta Crystallograph.,* 2008, vol. A64, pp. 112–122.

Zakharov, V.V., Chukanov, N.V., Dremova, N.N., Kazakov, A.I., Volkova, N.N., Chervonnyi, A.D., Korsounskii, B.L., and Shilov, G.V., High-temperature structural transformations of 1,1-diamino-2,2-dinitroethene (FOX-7), *Propellants, Explosives, Pyrotechnics*, 2016, vol. 41, pp. 2006–2012.

Zubkova, N.V., Pushcharovsky, D.Yu., Sarp, H., Teat, S.J., and MacLean, E.J., Crystal structure of zdenekite NaPbCu$_5$(AsO$_4$)$_4$Cl · 5H$_2$O *Crystallography Reports,* 2003, vol. 48, pp. 939–943.

Translated by I.A. Baksheev